



Open access

348

Views

3

CrossRef citations to date

0

Altmetric



Original Articles

# Dosimetric evaluation of scattered and attenuated radiation due to dental restorations in head and neck radiotherapy

Mona Azizi , Ali Asghar Mowlavi, Mahdi Ghorbani, Behnam Azadegan & Fatemeh Akbari

Pages 23-28 | Received 16 Jul 2017, Accepted 20 Oct 2017, Published online: 01 May 2019

 Download citation  <https://doi.org/10.1016/j.jrras.2017.10.004>



## Abstract

Formulae display:  **MathJax** 

In radiotherapy of head and neck cancer, the presence of high density materials modifies photon dose distribution near these high density materials during treatment. The aim of this study is to calculate the backscatter and attenuation effects of a healthy tooth, Amalgam, Ni-Cr alloy and Ceramco on the normal tissues before and after these materials irradiated by 6 and 15 MV photon beams, respectively. All measurements were carried out in a water phantom with dimension of  $50 \times 50 \times 50 \text{ cm}^3$  with an ionization chamber detector. Two points

In this article



ts after the dental sample were considered to score the photon  
e on the central beam axis was explored in a water phantom

absolute dose (cGy) was measured by prescription of 100 cGy dose in the water phantom at depth of 2.0 and 3.1 cm for 6 and 15 MV photons, respectively. At depth of 0.6 cm, the maximum percentage dose increase was observed with values of 6.99% and 9.43% for Ni-Cr and lowest percentage dose increase of 1.49% and 2.63% are related to the healthy tooth in 6 and 15 MV photon beams, respectively. The maximum absolute dose of 95.58 cGy and 93.64 cGy were observed at depth of 0.6 cm in presence of Ni-Cr alloy for 6 and 15 MV photon beams, respectively. The presence of dental restorations can cause backscattering dose during head and neck radiation therapy. Introduction of compositions and electron density of high density materials can improve the accuracy of dosimetric calculations in treatment planning systems to deliver the relevant dose to target organ and reduce the backscattering dose in healthy tissues in the surrounding of tooth.

**Q Keywords:** [Radiotherapy](#) [Dental restoration](#) [Dose distribution](#)

## 1 Introduction

One of important issues in radiotherapy of head and neck cancer is presence of dental restorations and implants. Among cancer patients with tumor in head and neck region, most of them have non-removable dental restorations. These high density materials cause perturbation in photon dose distribution in heterogeneous media when photon beam passes through these structures ([American dental association; Committee Task Group 63, 2003; Podgorsak, 2009](#)). During the radiotherapy, oral cavity and salivary glands are exposed to extra doses of this unwanted radiation. This dose increment increases the risk of some diseases such

radiotherapy (Hancock, Epstein, & Sadler, 2003; Nabil & Samman, 2012). This topic has been attended by the American Association of Physicists in Medicine (AAPM) Task Group, report No. 81, to investigate the subject of management of patients with high-Z materials (Reft et al., 2003).

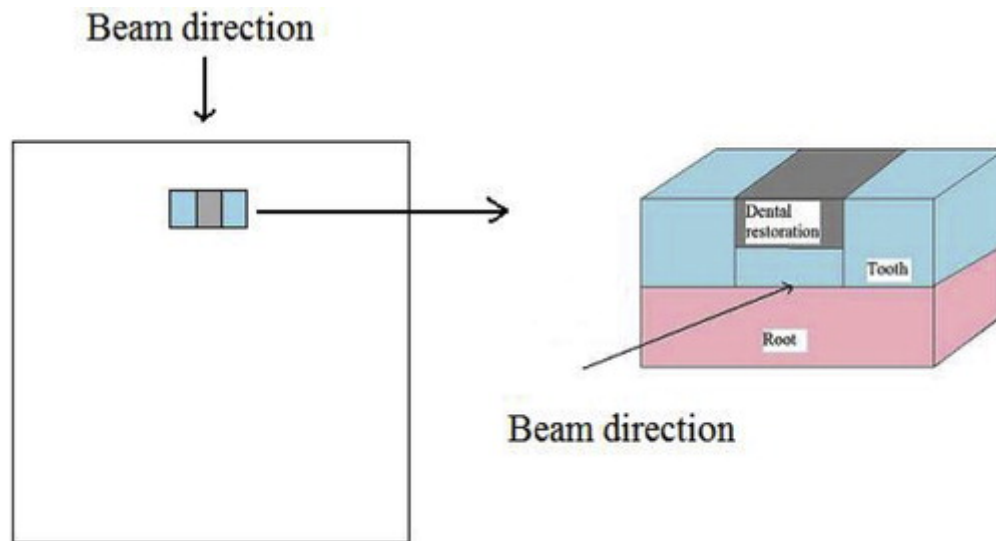
Several authors have quantitatively studied the effect of such dental restorations or high atomic number interfaces on photon dose distributions. Chang placed oral and bone phantom under 6 MV linac photon irradiation. He reported maximum and minimum backscatter dose of 53% and 10% due to presence of metal crown alloy and ceramic metal crown, respectively (Chang, Lin, Shiau, & Chie, 2014). In another study, Shimamoto investigated the dose scattering due to nine dental metals in a single-field technique, three-dimensional conformal radiation therapy (3D CRT), and intensity-modulated radiation therapy (IMRT). They placed radiochromic films on dental metals in a water phantom and irradiated them with 4 MV photon beam of Siemens medical accelerator. In the single-field technique the gold metal has the largest dose increase of 19.3% compared to the other dental metals whereas 3D CRT and IMRT had lower dose scattering than the single-field technique (Shimamoto et al., 2015). Furthermore, Catli studied the effect of pure titanium, titanium alloy, amalgam, and crown on dose distribution calculated with two methods: pencil beam convolution (PBC) algorithm and Monte Carlo simulation. A dose increase was seen due to electron backscattering in 2 cm at front of dental implant in tissue whereas Eclipse treatment planning system (TPS) did not account this backscattering radiation. Indeed, Eclipse underestimates the backscattered dose by the dental prostheses and overestimates the dose after these metals (Çatli, 2015). De Conto investigated 6 MV photon dose distribution due to dental restorations with Monte Carlo simulation and experimental measurement. Three samples including a healthy tooth, a tooth with Amalgam, and crown were irradiated in a

15 MV high energy photons to achieve the dose uniformity and deeper penetration. Therefore, this work focused on measurement of dose perturbations from high density materials in 6 and 15 MV medical photon beams. These commercial dental materials consist of tooth, tooth with Amalgam, tooth with Ni-Cr, and tooth with Ceramco.

## 2 Materials and methods

### 2.1 Dental samples

To evaluate photon dose distribution in presence of high density inhomogeneties in 6 and 15 MV photon beams of Siemens Primus medical linear accelerator (Siemens AG, Erlangen, Germany), three types of commercial dental materials were used. These commercial dental restorations which were considered independently in this study are a healthy tooth, tooth restored with Amalgam, tooth filled with Ni-Cr, and tooth with Ceramco. These samples were real healthy teeth which were collected randomly from dentistry clinics then were restored with frequent dentistry restoration materials. [Table 1](#) gives the physical densities, the compositions, the effective atomic numbers ( $Z$ ), electron density, electron density per gram, and electron density per  $\text{cm}^3$  of tooth and various restoration materials which were used in this study. These parameters will be used for more interpretation of 6 and 15 MV photon dose distribution.  $Z$  parameter is related to gama energy and it was calculated according to Mayneord formula ([Mayneord, 1937](#)). The dental phantom consists of the tooth filled partially with the dental restorations which were placed in the middle and two healthy teeth located in the both laterals. The dimensions of the healthy tooth are  $0.8 \times 1 \times 0.8 \text{ cm}^3$  which consists of 50% root and 50% dentine. For the restored teeth, almost 30% of their crown was made of commercial dental



Display full size

**Table 1 Weight fraction (%), effective atomic number, physical density ( $\text{g}/\text{cm}^3$ ) and electron density (number of electrons per  $\text{cm}^3$ ) for tooth ( Shved and Shishkina, 2000 ), Amalgam ( Chin et al., 2009 ), Ni-Cr alloy (General dentalsupply n.d.) and Ceramco ( Chin et al., 2009 ).**



CSV Display Table

## 2.2 In-phantom experimental measurements

Experimental measurements were performed by a Wellhofer-Scanditronix dosimetry system (Wellhofer, Uppsala, Sweden) at Reza Radiation Oncology Center (Mashhad, Iran). For in-phantom measurements, the dental phantom was placed in a water phantom (RFA-300; IBA Dosimetry GmbH, Schwarzenbruck, Germany) of  $50 \times 50 \times 50 \text{ cm}^3$  dimensions. To score the experimental data a Semiflex ionization chamber detector (PTW 31010 REF) with sensitive volume of  $0.125 \text{ cm}^3$  was used which was inserted in the water phantom.

In this article



▲ dental configurations in the water, a PMMA (Polymethyl  
 ▼ with  $1.18 \text{ g}/\text{cm}^3$  density was utilized due to its close density to

cancer, the dose was delivered with 6 and 15 MV X-ray beams so that the Z-axis, was perpendicular to the middle tooth sample. This measurement was repeated in the water phantom (open field) without dental sample. The irradiation purpose was to deliver 100 cGy at depth of 2.0 cm and 3.1 cm in water phantom for the 6 and 15 MV photon beams, respectively. This amount of dose corresponds to 101 monitor units (MU) for this kind of treatment unit. The field size had  $10 \times 10 \text{ cm}^2$  dimensions and source to surface distance (SSD) was 100 cm. To measure the photon dose, two points before and four points after the tooth were considered. These experimental set-up conditions were the same for all the dental configurations. Percentage dose increase (PDI) in each point with and without tooth and dental restorations was calculated by using the following formula:

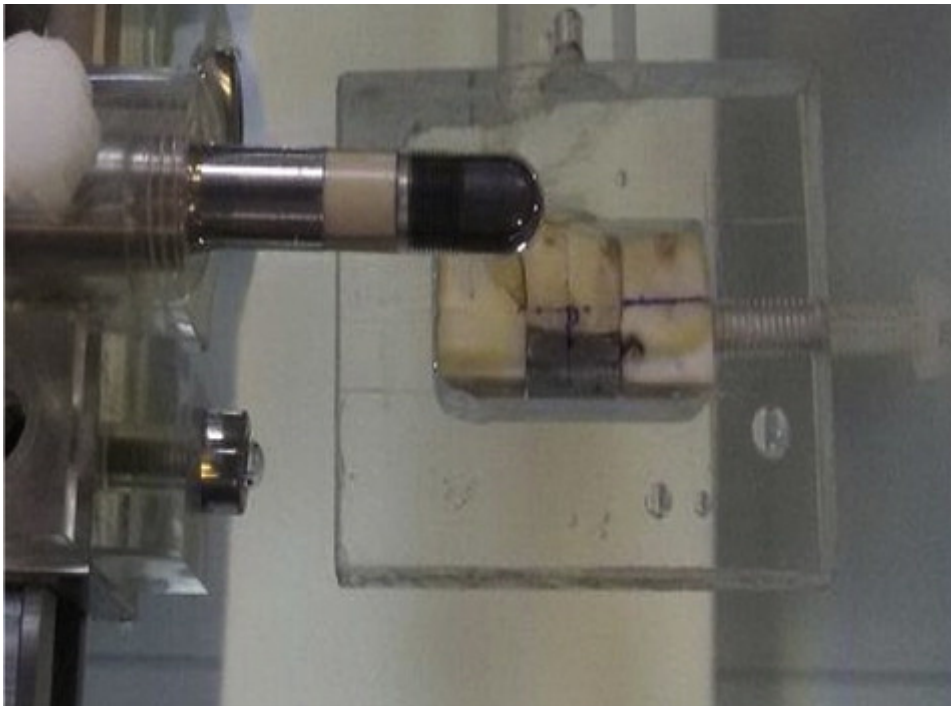
$$\text{Percentage dose increase} = ((D2-D1)/D1) \times 100$$

(1)

Where  $D$  and  $D$  imply photon dose in absence of sample (open field) and photon dose in presence of tooth dental restoration at the same certain point, respectively. The photon dose was measured at 2 points before the water-tooth interface (0.3 and 0.6 cm depths) and four points after the tooth-water interface (2.1, 2.6, 3.1 and 3.6 cm depths).

Fig. 2 Global view of dental samples with the holder in the water phantom and ionization chamber to the left picture.



[Display full size](#)

## 3 Results and discussion

### 3.1 Percentage dose increase in presence of dental restorations

In this study, the effect of tooth and three commercial dental restorations on photon dose distribution in head and neck radiotherapy with photon beams of a medical linac was evaluated. Dose backscattering and attenuation measurements due to the dental restorations along the 6 and 15 MV photon beam's central axes were performed by a dosimetry system (ionization chamber detector (PTW 31010 REF)). The values of the PDI in the case of tooth only, tooth with Amalgam, tooth with Ni-Cr alloy and tooth with Ceramco at different depths are listed in [Table 2](#). For further comparison, the results of 6 and 15 MV photon beams were presented for each phantom in [Fig. 3](#) and [Fig. 4](#), separately. The results of this study are consistent




MV photon beams. For all the four high density materials, the PDI increases with the depth in the water phantom up to the dental surface. In this area, the maximum PDI was found for Ni-Cr alloy, Amalgam, Ceramco, and tooth with values of 6.98%, 5.57%, 1.68%, and 1.49% relative to dose in water with 6 MV photon beam, respectively. This relative dose enhancement trend is also similarly observed for 15 MV photon beam with values of 9.43%, 7.82%, 5.04%, and 2.62% for Ni-Cr alloy, Amalgam, Ceramco, and tooth, respectively.

Fig. 3 Percentage dose increase (%) versus depth (cm) in the presence of tooth, tooth with Amalgam, tooth with Ni-Cr alloy and tooth with Ceramco, relative to dose in water for 6 MV photon beam.



Display full size

Fig. 4 Percentage dose increase (%) versus depth (cm) in the presence of tooth, tooth with Amalgam, tooth with Ni-Cr alloy and tooth with Ceramco, relative to dose

In this article  photon beam.



Display full size

**Table 2 Percentage dose increase (DIF) (%) in the presence of tooth, tooth with Amalgam, tooth with Ni-Cr alloy and tooth with Ceramco. The dental sample was placed at depth of 1 cm inside the water phantom for 6 and 15 MV photon beams.**



CSV Display Table

In photon therapeutic energies, the Compton scattering is the predominant process (Podgorsak and International Atomic Energy Agency, 2005). As 6 MV and 15 MV photon beams are nominal energies and made up an energy spectrum with maximum amounts up to 6 MV and 15 MV. In Compton scattering, high energy photons will deposit a larger fraction of their energy in tissue compared to low energy photons (William, 1994). Comparison of these variations for the healthy tooth and the three dental restorations are depicted in Fig. 4, where the 15 MV photon beam has higher PDI relative to 6 MV photons for all the high density materials. The maximum amount of PDI of 9.43% and 7.82% are observed for Ni-Cr

In this article



▲ 15 MV photon beam at depth of 0.6 cm, respectively. In this  
 ▼ values of 1.49% and 1.53% belong to the healthy tooth and

indicated that the physical density and electron density per  $\text{cm}^3$  have important roles in the backscattering dose, especially for higher energy photons. Previously some authors interpreted their results by effective atomic number (Chang, Hung, Chie, Shiau, & Huang, 2012; Friedrich, Todrovic, & Krull, 2010; Ozen et al., 2005; Shimosato et al., 2011). According to the data in Table 2, the largest backscattered dose is related to Ni-Cr alloy and Amalgam with electron density per  $\text{cm}^3$  of  $2.21 \times 10^{24}$  (number of electrons per  $\text{cm}^3$ ) and  $2.09 \times 10^{24}$  (number of electrons per  $\text{cm}^3$ ), respectively. However, the amount of electron density per  $\text{cm}^3$  of  $6.93 \times 10^{23}$  (number of electrons per  $\text{cm}^3$ ) and  $6.42 \times 10^{23}$  (number of electrons per  $\text{cm}^3$ ) of Ceramco and tooth cause a smaller back scattering dose increment.

The results in the present study are in agreement of the previous published researches (Chang et al., 2012; Reft et al., 2003). In these reports, they revealed that the Compton is strongly dependent on electron density per  $\text{cm}^3$  and is independent of  $Z$  (Khan, 2014). Amalgam and Ni-Cr alloy also include elements with high atomic number which have comparatively higher weight fractions (e.g. Amalgam includes 69.3% of Ag and Ni-Cr alloy includes 75% of Ni) whereas healthy tooth and Ceramco mainly consist of low atomic numbers and electron density per  $\text{cm}^3$ , respectively. Therefore, these high density materials cause a significant backscattering dose especially up to a few millimeters before the sample. This radiation backscattering can damage the healthy tissues before the inhomogeneities.

The second region is beyond the tooth sample, where the dose is attenuated after passing through the dental restoration materials. According to Figs. 3 and 4, for both 6 and 15 MV photon beams the PDI falls off in the first centimeters beyond the sample. At depth of 2.1 cm, because of backscattering and absorbing phenomena, Ni-Cr alloy and Amalgam have the lowest PDI of 15.37% and 10.53% for 6 MV photon beam, respectively. All data of the PDI which are listed in Table 2 signify that

Another practical quantity is absolute dose (cGy/100 Monitor Unit (MU)) which is measured by prescription of 100 cGy (100 MU) as the reference dose in open field (water) at depth of 2.1 cm and 3 cm for 6 and 15 MV photon beams, respectively. The results of the absolute dose in water and in presence of dental restorations are listed in [Table 3](#). In [Fig. 5](#) and [Fig. 6](#), it is observed that the absolute dose for all dental materials has more values compared to the water before the dental sample. In the 6 MV photon beam, the absolute dose for water was 85.89 cGy at 0.6 depth whereas the maximum values were observed for Ni-Cr alloy, Amalgam, Ceramco and tooth with amounts of 95.58 cGy, 92.87 cGy, 90.77 cGy and 89.29 cGy, respectively. It can also be observed for 15 MV photon that the trend of the absolute dose is similar to 6 MV photon beam. The highest absolute dose is related to Ni-Cr alloy and Amalgam with values of 93.64 cGy and 91.26 cGy compared to 78.20 cGy in water at 6.0 cm depth. By attention to [Table 3](#), in depth of 2.0 cm and 3.1 cm for 6 MV and 15 MV photon beams, it is found that for all the dental materials the absolute dose has the lower amounts compared to 100 cGy absolute dose for the open field. The maximum uncertainty of experimental measurements was 0.042%.

Fig. 5 Absolute dose (cGy) versus depth (cm) in the water and presence of tooth, tooth with Amalgam, tooth with Ni-Cr alloy and tooth with Ceramco, relative to dose in water for 6 MV photon beam.

[Display full size](#)

Fig. 6 Absolute dose (cGy) versus depth (cm) in the water and presence of tooth, tooth with Amalgam, tooth with Ni-Cr alloy and tooth with Ceramco, relative to dose in water for 15 MV photon beam.



[Display full size](#)

In this article



depth of 1 cm inside the water phantom for 6 and 15 MV photon beams. These results were measured in the case of prescription of 100 cGy (100 MU) at 2.0 cm and 3.1 cm depths for 6 MV and 15 MV photon beams.

CSV Display Table

The importance of the dosimetry calculations is indicated by the phenomenon of delivering unwanted dose to the healthy surrounding tissues around the high density materials and delivering reduced dose to the tumor cells. Delivery of excess dose to the healthy tissues before the high density materials and delivery of reduced dose to the target can be indicated the importance of dosimetry calculations. In a TPS only the electron densities of water, tissue and bone are considered as a standard reference dose in an external radiotherapy whereas the compositions and electron densities of high density materials and dental restorations are not taken into account.

## 4 Conclusion

Based on the results presented in this study, high density materials such as healthy tooth, tooth restored with Amalgam, tooth with Ni-Cr alloy, and tooth with Ceramco can perturb the photon dose distribution in radiotherapy of head and neck cancer. It should be noted that the dose perturbation decreases the accuracy of dosimetric calculation and have to be taken into account in treatment planning. In addition, the International Commission on Radiation Units and Measurements (ICRU) in report No. 24 emphasized that the uncertainty for dose delivery to target in radiotherapy should be in the range of  $\pm 5\%$  (Nath et al., 1995). The results of this research indicate that introduction of characteristics of high density materials such as

In this article



- ▲ electron density per  $\text{cm}^3$  in routine treatment planning
- 
- ▼ the accuracy of dosimetric calculations in the TPSs.

insignificant backscattering dose on healthy tissues before the sample. The overdose will be larger for the photon beam with higher energy for tumors which are localized in deeper regions. After these high density materials the presence of Ceramco can damage the normal tissue especially for the 15 MV photon beam. Using a low-Z material with appropriate thickness will shield effectively oral mucosa from excess dose.

## Notes

Peer review under responsibility of The Egyptian Society of Radiation Sciences and Applications.

## References

1. American dental association. General dental supply, <http://www.generaldentalsupply.com/thermabondv/>, Accessed 26 June 2015. [Google Scholar]
2. S. a. Berger W. Goldsmith R. A. Lewis Introduction to bioengineering 1996 Oxford University Press [Google Scholar]
3. S. Çatli High-density dental implants and radiotherapy planning: Evaluation of effects on dose distribution using pencil beam convolution algorithm and Monte Carlo method Journal of Applied and Clinical Medical Physics 16 2015 5612 [Crossref], [Web of Science ®], [Google Scholar]

different dental crowns and implants during LINAC photon irradiation *Radiation Physics and Chemistry* 1042014339344 [[Crossref](#)], [[Web of Science ®](#)], [[Google Scholar](#)]

6. D.W.Chin N.Treister B.Friedland R.A.Cormack R.B.Tishler G.M.Makrigiorgos Effect of dental restorations and prostheses on radiotherapy dose distribution: A Monte Carlo study *Journal of Applied and Clinical Medical Physics* 1020098089 [[Crossref](#)], [[Web of Science ®](#)], [[Google Scholar](#)]
7. Committee Task Group 63 *Medical Physics* 30200311621182 [[Crossref](#)], [[Web of Science ®](#)], [[Google Scholar](#)]
8. D.C.Conto R.Gschwind E.Martin L.Makovicka Study of dental prostheses influence in radiation therapy *Physica Medica* 302014117121 [[Crossref](#)], [[Web of Science ®](#)], [[Google Scholar](#)]
9. M.Farahani F.C.Eichmiller Metal polysiloxane shields for radiation therapy of maxilla-facial tumors *Medical Physics* 181991273276 [[Crossref](#)], [[Web of Science ®](#)], [[Google Scholar](#)]
10. R.E.Friedrich M.Todrovic A.Krull Simulation of scattering effects of irradiation on surroundings using the example of titanium dental implants: A Monte Carlo approach *Anticancer Research* 30201017271730 [[Web of Science ®](#)], [[Google Scholar](#)]
11. P.J.Hancock J.B.Epstein G.R.Sadler Oral and dental management related to radiation therapy for head and neck cancer *Journal of the Canadian Dental*



13. R. LeoWilliamTechniques for nuclear and particle physics experiments2nd ed.1994Springer verlag [\[Google Scholar\]](#)
  
14. W.V.MayneordThe significance of the roentgenActa Union Int Contre Cancer21937271282 [\[Google Scholar\]](#)
  
15. S.NabilN.SammanRisk factors for osteoradionecrosis after head and neck radiation: A systematic reviewOral Surgery, Oral Medicine, Oral Pathology and Oral Radiology11320125469 [\[Crossref\]](#), [\[Web of Science ®\]](#), [\[Google Scholar\]](#)
  
16. R.1NathL.L.AndersonG.LuxtonK.A.WeaverJ.F.WilliamsonA.S.MeigooniDosimetry of interstitial brachytherapy sources: Recommendations of the AAPM radiation therapy committee task group No. 43 american association of Physicists in medicineMedical Physics221995209234 [\[Crossref\]](#), [\[Web of Science ®\]](#), [\[Google Scholar\]](#)
  
17. J.OzenB.DiricanK.OysulM.BeyzadeogluO.UcokB.BeydemirDosimetric evaluation of the effect of dental implants in head and neck radiotherapyOral Surgery, Oral Medical, Oral Pathology and Oral Radiology992005743747 [\[Crossref\]](#), [\[Web of Science ®\]](#), [\[Google Scholar\]](#)
  
18. E.B.PodgorsakRadiation physics for medical physicist2<sup>nd</sup> ed.2009Springer [\[Google Scholar\]](#)
  
19. E.D.PodgorsakInternational Atomic Energy Agency. Radiation oncology physics: A handbook for teachers and studentsInternational Atomic Energy Agency2005 [\[Google Scholar\]](#)

21. C.ReftR.AlecuI.J.DasB.J.GerbiP.KeallE.Liefet alDosimetric considerations for patients with HIP prostheses undergoing pelvic irradiation. Report of the AAPM radiation therapy,committee task group 63Medical Physics30200311621182  
[\[Crossref\]](#), [\[Web of Science ®\]](#), [\[Google Scholar\]](#)
  
22. B.ReitemeierG.ReitemeierA.SchmidtW.SchaalP.BlochbergerEvaluation of a device for attenuation of electron release from dental restorations in a therapeutic radiation fieldJournal of Prosthetic Dentistry872002323327  
[\[Crossref\]](#), [\[Web of Science ®\]](#), [\[Google Scholar\]](#)
  
23. R.RussellK.PillaiP.K.JonesIn vitro backscattering from implant materials during radiotherapyJournal of Prosthetic Dentistry751996626632  
[\[Crossref\]](#), [\[Web of Science ®\]](#), [\[Google Scholar\]](#)
  
24. H.ShimamotoI.SumidaN.KakimotoK.MarutaniR.OkahataA.Usamiet alEvaluation of the scatter doses in the direction of the buccal mucosa from dental metalsJournal of Applied and Clinical Medical Physics1620155374 [\[Crossref\]](#), [\[Web of Science ®\]](#) , [\[Google Scholar\]](#)
  
25. T.ShimozatoY.IgarashiY.ItohN.YamamotoK.OkudairaK.Tabushiet alScattered radiation from dental metallic crowns in head and neck radiotherapyPhysics in Medicine and Biology56201155255534 [\[Crossref\]](#), [\[Web of Science ®\]](#), [\[Google Scholar\]](#)
  
26. V.A.ShvedE.A.ShishkinaAssessment of tooth tissues dose rate coefficients from incorporated strontium-90 in EPR dose reconstruction for the Techa Riverside populationHarmonization of radiation, human life and the ecosystem,